Article

Molecular Squares with Paramagnetic Diruthenium Corners: Synthetic and Crystallographic Challenges

Panagiotis Angaridis, John F. Berry, F. Albert Cotton, Carlos A. Murillo, and Xiaoping Wang

J. Am. Chem. Soc., **2003**, 125 (34), 10327-10334• DOI: 10.1021/ja036095x • Publication Date (Web): 22 July 2003

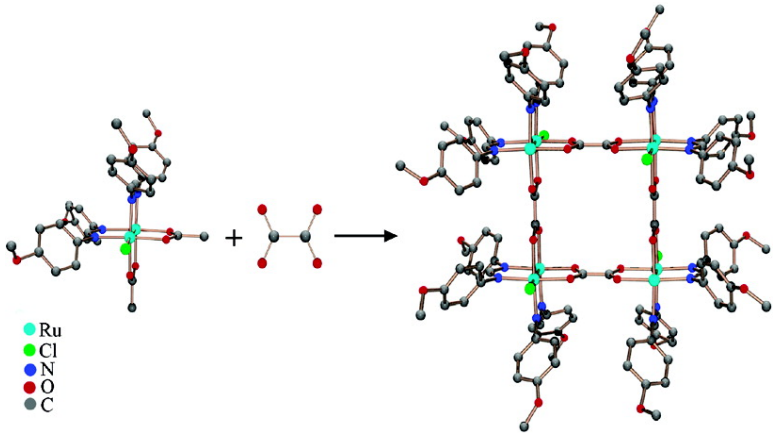

More About This Article

Additional resources and features associated with this article are available within the HTML version:

- Supporting Information
- Links to the 12 articles that cite this article, as of the time of this article download
- Access to high resolution figures
- Links to articles and content related to this article
- Copyright permission to reproduce figures and/or text from this article

View the Full Text HTML

J|A|C|S
ARTICLES
Published on Web 07/22/2003

Molecular Squares with Paramagnetic Diruthenium Corners: Synthetic and Crystallographic Challenges

Panagiotis Angaridis, John F. Berry, F. Albert Cotton,* Carlos A. Murillo,* and Xiaoping Wang

Contribution from the Department of Chemistry and Laboratory for Molecular Structure and Bonding, P.O. Box 30012, Texas A&M University, College Station, Texas 77842−3012

Received May 12, 2003; E-mail: cotton@tamu.edu; murillo@tamu.edu

Abstract: The reaction of $Ru_2(\mu\text{-}O_2CMe)_4Cl$ with ∼2.5 equiv of HDAniF (HDAniF = *N*,*N*′-di(*p*-anisyl)-formamidine) in refluxing THF resulted in the synthesis of *cis*-$Ru_2(\mu\text{-DAniF})_2(\mu\text{-}O_2CMe)_2Cl$ (**1**). This Ru_2^{5+}-complex, which has two labile acetate groups occupying two equatorial *cisoid* positions, was used for the construction of discrete paramagnetic supramolecular arrays. Subsequent reactions of **1** with HO_2C-CO_2H (oxalic acid) and 1,4-$HO_2C-C_6H_4-CO_2H$ (terephthalic acid) followed by recrystallization from 1,2-$C_2H_4Cl_2$/hexanes solutions containing wet MeCN or 4-Bu^{t}py (4-*tert*-butylpyridine) gave crystals of $[\{cis\text{-}Ru_2(\mu\text{-DAniF})_2Cl(H_2O)\}(\mu\text{-oxalate})]_4\cdot MeCN\cdot 2(C_6H_{14})\cdot 12(H_2O)$ (**2**) and $[\{cis\text{-}Ru_2(\mu\text{-DAniF})_2Cl_{0.646}(4\text{-Bu}^t\text{py})_{1.354}\}(\mu\text{-terephthlate})]_4Cl_{1.414}\cdot 17(1,2\text{-}C_2H_4Cl_2)\cdot C_6H_{14}$ (**3**), respectively. These are the first polygonal supramolecular assemblies consisting of paramagnetic M_2 units at each apex, where $M_2 = Ru_2^{5+}$. Compounds **2** and **3** have been structurally characterized, and their electrochemistry and magnetic properties have been studied. These studies have confirmed that oxalate linkers are better than the terephthalate linkers in effecting electronic and magnetic coupling.

Introduction

The formation of metal-containing supramolecular entities by assembly of constituents in solution continues to be a topic of great interest.[1] By using mononuclear units, such as $M(amine)_2^{2+}$ (M = Pd, Pt) and other similar entities as corner pieces, connected by appropriate linkers such as 4,4′-bipyridine, diverse polygonal molecules have been synthesized, which are often highly charged (Scheme 1a).[2] We have pioneered the use of metal−metal bonded dinuclear units of the type *cis*-$M_2(\mu\text{-DAniF})_2$ (DAniF = the anion of *N*,*N*′-di(*p*-anisyl)formamidine, M = Mo and Rh) and dicarboxylate anions as linkers (Scheme 1b).[3] This leads to neutral products, which are often redox active, and, depending on the nature of the linker, communication between the dimetal units through the linker has been detected by electrochemical means. So far, a few molecular squares have been structurally characterized for Mo[4,5] and Rh,[6] a more limited number of triangles for M = Mo,[7] Rh[4] and Re,[8] all derived from the well-known paddlewheel motif, as well as a series of

Scheme 1

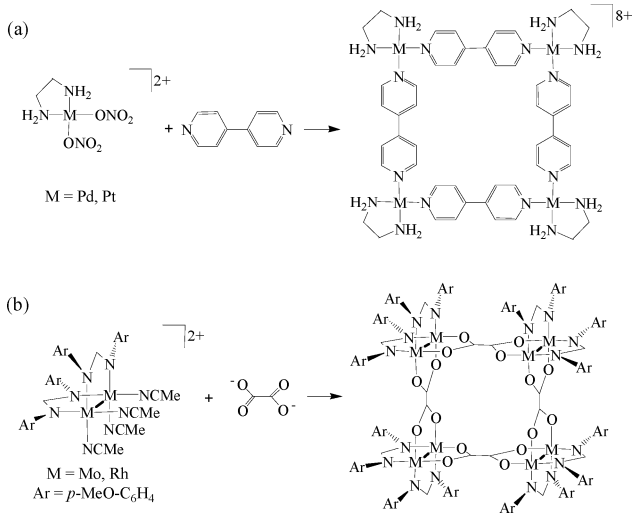

(1) Lehn, J.-M. *Supramolecular Chemistry*; VCH Publishers: New York, 1995.
(2) (a) Leininger, S.; Olenyuk, B.; Stang, P. J. *Chem. Rev.* **2000**, *100*, 853 and references therein. (b) Swiegers, G. F.; Malefetse, T. J. *Chem. Rev.* **2000**, *100*, 3483. (c) Fujita, M. *Chem. Soc. Rev.* **1998**, *27*, 417 and references therein. (d) Espinet, P.; Soulantica, K.; Charmant, J. P. H.; Orpen, A. G. *Chem. Commun*. **2000**, 915. (e) Navarro, J. A. R.; Lippert, B. *Coord. Chem. Rev.* **1999**, *185*−*186*, 653. (f) Whang, D.; Kim, K. *J. Am. Chem. Soc*. **1997**, *119*, 451. (g) Mann, S.; Huttner, G.; Zsolnai, L.; Heinze, K. *Angew. Chem., Int. Ed. Engl.* **1996**, *35*, 2808. (h) Scherer, M.; Caulder, D. L.; Johnson, D. W.; Raymond, K. N. *Angew. Chem., Int. Ed.* **1999**, *38*, 1588. (i) Lai, S.-W.; Chan, M. C.-W.; Peng, S.-M.; Che, C.-M. *Angew. Chem., Int. Ed.* **1999**, *38*, 669. (j) Jones, C. J. *Chem. Soc. Rev.* **1998**, *27*, 289. (k) Klausmeyer, K. K.; Wilson, S. R.; Rauchfuss, T. B. *J. Am. Chem. Soc.* **1999**, *121*, 2705. (l) Li, H.; Eddaoudi, M.; O'Keeffe, M.; Yaghi, O.-M. *Nature* **1999**, *402*, 276.
(3) (a) Cotton, F. A.; Lin, C.; Murillo, C. A. *Acc. Chem. Res*. **2001**, *34*, 759. (b) Cotton, F. A.; Lin, C.; Murillo, C. A. *Proc. Natl. Acad. Sci. U.S.A.* **2002**, *99*, 4810.
(4) Cotton, F. A.; Daniels, L. M.; Lin, C.; Murillo, C. A. *J. Am. Chem. Soc*. **1999**, *121*, 4538.
(5) Cotton, F. A.; Lin, C.; Murillo, C. A. *Inorg. Chem*. **2001**, *40*, 478.
(6) (a) Cotton, F. A.; Lin, C.; Murillo, C. A.; Yu, S.-Y. *J. Chem. Soc., Dalton Trans*. **2001**, 502. (b) Schiavo, S. L.; Pocsfalvi, G.; Serroni, S.; Cardiano, P.; Piraino, P. *Eur. J. Inorg. Chem*. **2000**, 1371. (c) Bonar-Law, R. P.; McGrath, T. D.; Singh, N.; Bickley, J. F.; Steiner, A. *Chem. Commun*. **1999**, 2457. (d) Bickley, J. F.; Bonar-Law, R. P.; Femoni, C.; MacLean, E. J.; Steiner, A.; Teat, S. J. *J. Chem. Soc., Dalton Trans*. **2000**, 4025.
(7) Cotton, F. A.; Lin, C.; Murillo, C. A. *Inorg. Chem*. **2001**, *40*, 575.
(8) For rhenium, the corner piece is composed of *cis*-$Re_2(\mu\text{-dppm})_2Cl_2^{2+}$ units and terephthalate dianions. See: Bera, J. K.; Angaridis, P.; Cotton, F. A.; Petrukhina, M. A.; Fanwick, P. E.; Walton, R. A. *J. Am. Chem. Soc.* **2001**, *123*, 1515.

isomeric triangles where the corner piece is $L_2Ru_2(CO)_4$, L = *ax*-MeCN or *ax*-PPh_3, and the linker is the anion of tartaric acid.[9] Recently, Shiu et al. have used the same Ru_2-carbonyl corner piece to make a square and a loop using oxalate and malonate as linkers.[10]

The common characteristic of all of the aforementioned molecular macrocycles is that they are based on closed-shell dimetal units and are diamagnetic. However, there are also dimetal units with odd numbers of electrons which are paramagnetic. The use of paramagnetic dimetal building blocks in the construction of supramolecular arrays offers the opportunity to synthesize paramagnetic macrocyclic assemblies and study their magnetic behavior. It should be noted that the rational design of paramagnetic assemblies in the context of supramolecular chemistry has been difficult to achieve. Simple triangular systems have been the most well studied,[11] although a few more complex systems are known.[12] To achieve a general and rational design of paramagnetic entities with dimetal building blocks, Ru_2 units are most appealing, because they can exhibit different magnetic properties depending on the oxidation state and the type of the bridging ligands embracing the Ru_2 unit.[13] For example, Ru_2^{5+}-tetraformamidinate compounds have the electronic configuration $\sigma^2\pi^4\delta^2\pi^{*2}\delta^{*1}$ with $S = {}^3/_2$ (the π^* and δ^* molecular orbitals are essentially degenerate), while the analogous complexes of the Ru_2^{4+} core have the electronic configuration $\sigma^2\pi^4\delta^2(\pi^*)^4$ and they are diamagnetic.

Because of the strong axial zero-field splitting exhibited by Ru_2^{5+} compounds, supramolecules incorporating the Ru_2^{5+} unit are desirable as potential single molecule magnets.[14] Some supramolecular assemblies based on Ru_2 units have been synthesized in the past, but they have been either oligomeric or polymeric one-dimensional chains,[15] or two- and three-dimensional networks[14,16] based on the coordination of linkers to the axial positions of the Ru_2 units. Discrete macrocyclic assemblies constructed using equatorial linkers and paramagnetic Ru_2 units have never been reported in the literature. This paper reports the results of our efforts in this direction. We describe the synthesis and characterization of a Ru_2^{5+} complex that is a building block of the first paramagnetic square macrocyclic assemblies based on Ru_2^{5+} corner pieces and dicarboxylate linkers. In addition, the structural, electrochemical, and magnetic properties of the resulting square macrocycles are discussed.

Results and Discussion

One of the most important considerations when designing the synthesis of supramolecular assemblies is to have readily accessible or, at least, easily prepared building blocks. Therefore, much effort was put into the quest for a precursor of Ru_2 building blocks, that is, a suitable Ru_2 complex with a mixed set of labile and nonlabile equatorial ligands.

Previous work from our laboratory has shown that *N*,*N*′-donor bridging ligands, for example, formamidinates, are particularly good as nonlabile ligands stabilizing Ru_2 units, while the acetate groups have shown their ability to act as labile ligands in many cases.[13] In addition, it has been reported recently that Ru_2^{5+} complexes with a mixed set of admp/$MeCO_2^-$ ligands of the type $Ru_2(\mu\text{-admp})_{4-n}(\mu\text{-}O_2CMe)_nCl$ (n = 0, 1, 2, 3, and admp = the anion of 2-amino-4,6-dimethylpyridine) can be selectively synthesized by careful control of the temperature of the reaction of $Ru_2(\mu\text{-}O_2CMe)_4Cl$ with Hadmp.[17] We thought that by studying the analogous substitution reactions of $Ru_2(\mu\text{-}O_2CMe)_4Cl$ with formamidines and by varying the experimental conditions (temperature, time, solvent, ratio of reactants), it might be possible to synthesize Ru_2^{5+} complexes with mixed sets of formamidinate/acetate ligands in a selective manner. Considerable exploratory work was conducted, and a variety of Ru_2^{5+} complexes were isolated as will be reported elsewhere.[18] Here will be discussed only the regiospecific synthesis of one Ru_2^{5+} complex, *cis*-$Ru_2(\mu\text{-DAniF})_2(\mu\text{-}O_2CMe)_2Cl$ (**1**), which has opened up the entire chemistry of paramagnetic supramolecular arrays.

The key molecule, **1**, was isolated as a green-purple solid from the reaction of $Ru_2(\mu\text{-}O_2CMe)_4Cl$ with ~2.5 equiv of HDAniF in refluxing THF for 24 h. It is the first mixed formamidinate/acetate complex having a *cisoid* arrangement of bridging ligands around the Ru_2^{5+} core. In most reactions of $Ru_2(\mu\text{-}O_2CMe)_4Cl$ with *N*,*O*-, or *N*,*N*′-donor bridging ligands (such as hydroxypyridines, aminopyridines, or formamidines) that result in the substitution of only two acetate groups, the inserted ligands occupy *transoid* positions.[19] To our knowledge, there are only two Ru_2 complexes in which the substituting ligands are found in *cisoid* positions, and they are both complexes of the Ru_2^{4+} core. One of them is [*cis*-$Ru_2(\mu\text{-pynp})_2(\mu\text{-}O_2CMe)_2](PF_6)_2$ (pynp = 2-(2-pyridyl)-1,8-naphthyridine),[20] and the other one is [*cis*-$Ru_2(\mu\text{-9-EtGH})_2(\mu\text{-}O_2CMe)_{2-x}(\mu\text{-}O_2CCF_3)_x(MeOH)_2](O_2CCF_3)_2$ (x = 0.18, and 9-EtGH = 9-ethylguanine).[21] The procedure used for the synthesis of **1** can be extended so that *cis*-substituted species with other formamidinate complexes can also be synthesized. In fact, the similar complex *cis*-$Ru_2(\mu\text{-DTolF})_2(\mu\text{-}O_2CMe)_2Cl$ (DTolF = *N*,*N*′-di(*p*-tolyl)-formamidinate) has also been structurally characterized from an analogous reaction of $Ru_2(\mu\text{-}O_2CMe)_4Cl$ with HDTolF.[22]

The use of **1** as a Ru_2^{5+} building block for supramolecular arrays was tested in carboxylate exchange reactions with two linear dicarboxylic acids: HO_2C-CO_2H and

(9) Süss-Fink, G.; Wolfender, J.-L.; Neumann, F.; Stoeckli-Evans, H. *Angew. Chem., Int. Ed. Engl.* **1990**, *29*, 429.
(10) Shiu, K.-B.; Lee, H.-C.; Lee, G.-H.; Wang, Y. *Organometallics* **2002**, *21*, 4013.
(11) See, for example: (a) López-Sandoval, H.; Coutreras, R.; Escuer, A.; Vicente, R.; Bernès, S.; Nöth, H.; Leigh, G. J.; Barba-Behrens, N. *J. Chem. Soc., Dalton Trans.* **2002**, 2648. (b) Raptopoulou, C. P.; Tangoulis, V.; Psycharis, V. *Inorg. Chem.* **2000**, *39*, 4452. (c) Du, M.; Bu, X.-H.; Guo, Y.-M.; Zhang, L.; Liao, D.-Z.; Ribas, J. *Chem. Commun.* **2002**, 1478.
(12) See, for example: (a) Campos-Fernández, C. S.; Clérac, R.; Koomen, J. M.; Russell, D. H.; Dunbar, K. R. *J. Am. Chem. Soc.* **2001**, *123*, 773. (b) Liu, X.; McAllister, J. A.; de Miranda, M. P.; Whitaker, B. J.; Kilner, C. A.; Thornton-Pett, M.; Halcrow, M. A. *Angew. Chem., Int. Ed.* **2002**, *41*, 756. (c) Michaut, C.; Ouahab, L.; Bergerat, P.; Kahn, O.; Bousseksou, A. *J. Am. Chem. Soc.* **1996**, *118*, 3610. (d) Kahn, O. *Acc. Chem. Res.* **2000**, *33*, 647.
(13) Cotton, F. A.; Walton, R. A. *Multiple Bonds Between Metal Atoms*, 2nd ed.; Oxford University Press: Cambridge, MA, 1988.
(14) Liao, Y.; Shum, W. W.; Miller, J. S. *J. Am. Chem. Soc.* **2002**, *124*, 9336.
(15) (a) Cotton, F. A.; Kim, Y.; Ren, T. *Inorg. Chem.* **1992**, *31*, 2723. (b) Wesemann, J. L.; Chisholm, M. H. *Inorg. Chem.* **1997**, *36*, 3258. (c) Wong, K.-T.; Lehn, J.-M.; Peng, S.-M.; Lee, G.-H. *Chem. Commun.* **2000**, 2259.
(16) (a) Miyasaka, H.; Campos-Fernández, C. S.; Clérac, R.; Dunbar, K. R. *Angew. Chem., Int. Ed.* **2000**, *39*, 3831. (b) Yi, X.-Y.; Zheng, L.-M.; Xu, W.; Feng, S. *Inorg. Chem.* **2003**, *41*, 2827.
(17) Cotton, F. A.; Yokochi, A. *Inorg. Chem.* **1998**, *37*, 2723.
(18) Angaridis, P.; Cotton, F. A.; Murillo, C. A., unpublished results.
(19) (a) Chakravarty, A. R.; Cotton, F. A. *Inorg. Chim. Acta* **1985**, *105*, 19. (b) Chakravarty, A. R.; Tocher, D. A.; Cotton, F. A. *Inorg. Chem.* **1985**, *24*, 2857. (c) Ren, T.; DeSilva, V.; Zou, G.; Lin, C.; Daniels, L. M.; Campana, C. F.; Alvarez, J. C. *Inorg. Chem. Commun.* **1999**, *2*, 301.
(20) Campos-Fernández, C. S.; Thomson, L.; Galán-Mascarós, J. R.; Ouyang, X.; Dunbar, K. R. *Inorg. Chem.* **2002**, *41*, 1523.
(21) Crawford, C. A.; Day, E. F.; Saharan, V. P.; Folting, K.; Huffman, J. C.; Dunbar, K. R.; Christou, G. *Chem. Commun.* **1996**, 1113.

1,4-$HO_2C-C_6H_4-CO_2H$. The reactions were carried out in refluxing toluene for 2 days, resulting in the substitution of the acetate groups of **1** by the dicarboxylates and the formation of square macrocyclic assemblies, isolated as purple-brown precipitates, according to the following general equation:

$$4cis\text{-}Ru_2(\mu\text{-DAniF})_2(\mu\text{-}O_2CMe)_2Cl + 4HL{-}LH \rightarrow [\{cis\text{-}Ru_2(\mu\text{-DAniF})_2Cl\}(\mu\text{-L}{-}L)]_4 + 8MeCO_2H$$

$$L{-}L = O_2C{-}CO_2,\ 1,4\text{-}O_2C{-}C_6H_4{-}CO_2$$

These solids are air-stable, while their dilute solutions in organic solvents are air-sensitive. Surprisingly, the crystallization of the resulting molecular squares proved to be very difficult, and many variables had to be tested. Diffusion of hexanes into $1,2\text{-}C_2H_4Cl_2$ solutions of the compounds gave the best crystals. In the presence of H_2O and MeCN, the oxalate square gave crystals with composition $[\{cis\text{-}Ru_2(\mu\text{-DAniF})_2Cl(H_2O)\}(\mu\text{-oxalate})]_4 \cdot MeCN \cdot 2(C_6H_{14}) \cdot 12(H_2O)$ (**2**), while the terephthalate analogue was crystallized in the presence of 4-Bu^{t}py as $[\{cis\text{-}Ru_2(\mu\text{-DAniF})_2Cl_{0.646}(4\text{-}Bu^tpy)_{1.354}\}(\mu\text{-terephthlate})]_4Cl_{1.414} \cdot 17\text{-}(1,2\text{-}C_2H_4Cl_2) \cdot C_6H_{14}$ (**3**). The oxalate square did not crystallize from solutions containing pyridines, while the terephthalate square did not form crystals when wet MeCN was present. Whenever $1,2\text{-}C_2H_4Cl_2$ was substituted by CH_2Cl_2, the diffraction quality of the crystals was greatly diminished, and other common solvents such as THF yielded only amorphous solids. The crystals lose solvent readily, and handling had to be minimized whenever intact single crystals were needed. According to TGA measurements, solvent loss begins at once at room temperature and continues steadily, with a few poorly defined breaks, up to 275 °C, after which rapid decomposition occurs.

Crystal Structures. Complex **1** crystallized in the monoclinic space group $P2_1/n$ with four molecules in the unit cell. A thermal ellipsoid drawing of **1** is shown in Figure 1, and selected bond distances and angles are listed in Table 1. Its molecular structure consists of two Ru atoms spanned by two bridging DAniF and two $MeCO_2^-$ ligands at *cisoid* positions. The Ru(1)−Ru(2) bond distance is 2.319(1) Å. This is midway between those commonly found for $Ru_2(\mu\text{-}O_2CR)_4Cl$ complexes which fall in the narrow range of 2.27−2.29 Å,[23] and those of the Ru_2(formamidinate)$_4$Cl complexes which vary over the range 2.34−2.39 Å.[24] The average of the Ru−N bond lengths is 2.030[4] Å, while the average of the Ru−O bond lengths is 2.068[4] Å. The Ru−O distances are elongated as compared to those in Ru_2(carboxylate)$_4$Cl (1.98−2.02 Å), and this elongation can be attributed to the strong *trans* effect of the DAniF ligands. The axially coordinated Cl^- is at a distance of 2.4861(7) Å from Ru(1). The Ru(2)−Ru(1)−Cl angle is 170.61(2)°, with the Cl^- tilted toward the two acetate groups, apparently due to the steric demand of the DAniF ligands. A water molecule was found in the vicinity of the other axial position of the Ru_2^{5+} unit at a distance of 2.495(3) Å from Ru(2), with a Ru(1)−Ru(2)···O angle of 165.2(6)°.

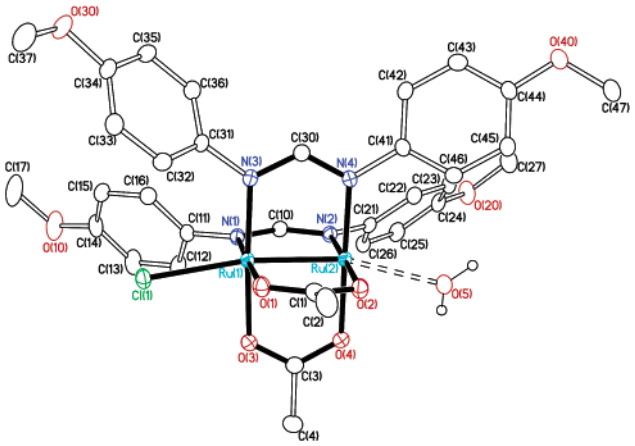

Figure 1. A perspective view of **1** with the atoms represented by thermal ellipsoids at the 35% probability level. Hydrogen atoms, except for those of the H_2O molecule, are omitted for clarity.

Table 1. Selected Bond Distances (Å) and Angles (deg) for **1**

Ru(1)−Ru(2)	2.319(1)	Ru(2)−N(2)	2.035(2)
Ru(1)−N(1)	2.034(2)	Ru(2)−N(4)	2.022(2)
Ru(1)−N(3)	2.028(2)	Ru(2)−O(2)	2.067(2)
Ru(1)−O(1)	2.072(2)	Ru(2)−O(4)	2.058(2)
Ru(1)−O(3)	2.075(2)	Ru(2)···O(5)	2.495(3)
Ru(1)−Cl(1)	2.486(7)		
N(1)−Ru(1)−N(3)	92.94(8)	O(2)−Ru(2)−O(4)	89.52(7)
N(1)−Ru(1)−O(1)	178.47(8)	N(1)−Ru(1)−Ru(2)	90.35(6)
N(1)−Ru(1)−O(3)	176.61(8)	O(1)−Ru(1)−Ru(2)	88.12(5)
N(3)−Ru(1)−O(3)	176.61(8)	O(1)−Ru(1)−Cl(1)	87.63(5)
N(3)−Ru(1)−O(1)	86.98(8)	O(3)−Ru(1)−Cl(1)	84.20(5)
O(1)−Ru(1)−O(3)	90.81(7)	Ru(2)−Ru(1)−Cl(1)	170.61(2)
N(2)−Ru(2)−N(4)	93.85(9)	Ru(1)−Ru(2)···O(5)	165.2(6)

The core structures of **2** and **3** are similar to each other, and they consist of four $cis\text{-}Ru_2(\mu\text{-DAniF})_2^{3+}$ units which are connected by dicarboxylate linkers (oxalate and terephthalate, respectively) forming square macrocycles (Figure 2). Complex **2** crystallized in the tetragonal space group $I4/m$, with 2 molecules in the unit cell together with 1 MeCN, 2 hexane and 12 H_2O molecules. It resides on a special position with D_{4h} symmetry. Only one-half of each apical Ru_2^{5+} unit and the $4/m$ symmetry operations generate the whole molecule. Crystals of complex **3** conform to the triclinic space group $P\bar{1}$. The molecule resides on a crystallographic inversion center, and only two of the four Ru_2^{5+} units are found in the asymmetric unit. It cocrystallized with 1 hexane and 17 $1,2\text{-}C_2H_4Cl_2$ molecules. Selected interatomic distances and angles for **2** and **3** are listed in Tables 2 and 3, respectively. The Ru−Ru distances are 2.332(2) Å for **2** and 2.3323(7) and 2.3247(7) Å for the two crystallographically independent Ru_2^{5+} units in **3**. These are very similar to that of 2.3192(3) Å in **1**. The Ru−Cl bond distance is 2.443(6) Å for **2**, and in the range 2.528(2)−2.576(7) Å for **3**. Again, these distances are similar to that in **1**.

The previously isolated molecular macrocycles based on multiply bonded dimetal building blocks contain one of the closed-shell Rh_2^{4+}, Mo_2^{4+}, or Re_2^{6+} units. In those cases, there have been either no axial ligands (Mo_2^{4+}) or, with rare

(22) The complex that was structurally characterized was $cis\text{-}Ru_2(\mu\text{-DTolF})_2(\mu\text{-}O_2CMe)_2Cl(HN{=}CH{-}NH{-}C_6H_4{-}p\text{-Me})$. The axially coordinated HN=CH−NH−C_6H_4−*p*-Me is an impurity which was initially present in the HDTolF used as starting material for the reaction (probably due to decomposition). Crystal data: $cis\text{-}Ru_2(\mu\text{-DTolF})_2(\mu\text{-}O_2CMe)_2Cl(HN{=}CH{-}NH{-}C_6H_4{-}p\text{-Me}) \cdot 2CH_2Cl_2$, $C_{44}H_{49}Cl_5N_6O_4Ru_2$, FW 935.48 space group $P1$, $a = 10.0476(5)$ Å, $b = 15.2900(8)$ Å, $c = 17.840(1)$ Å, $\alpha = 69.177(1)°$, $\beta = 89.916(1)°$, $\gamma = 74.787(1)°$, $V = 2459.1$ Å^3, $Z = 2$. Intensity data were collected on a BRUKER SMART 1000 area detector system at −60 °C. A total number of 12 962 independent reflections were measured, of which 11 178 were observed ($I > 2\sigma(I)$). The structure was solved by direct methods using SHELXTL and refined using SHELXL-97. Final full-matrix least squares refinement converged to R1 = 0.0375 and wR2 = 0.0831 for data with $I > 2\sigma(I)$.

(23) Aquino, M. A. S. *Coord. Chem. Rev.* **1998**, *170*, 141.

(24) Ren, T. *Coord. Chem. Rev.* **1998**, *175*, 43.

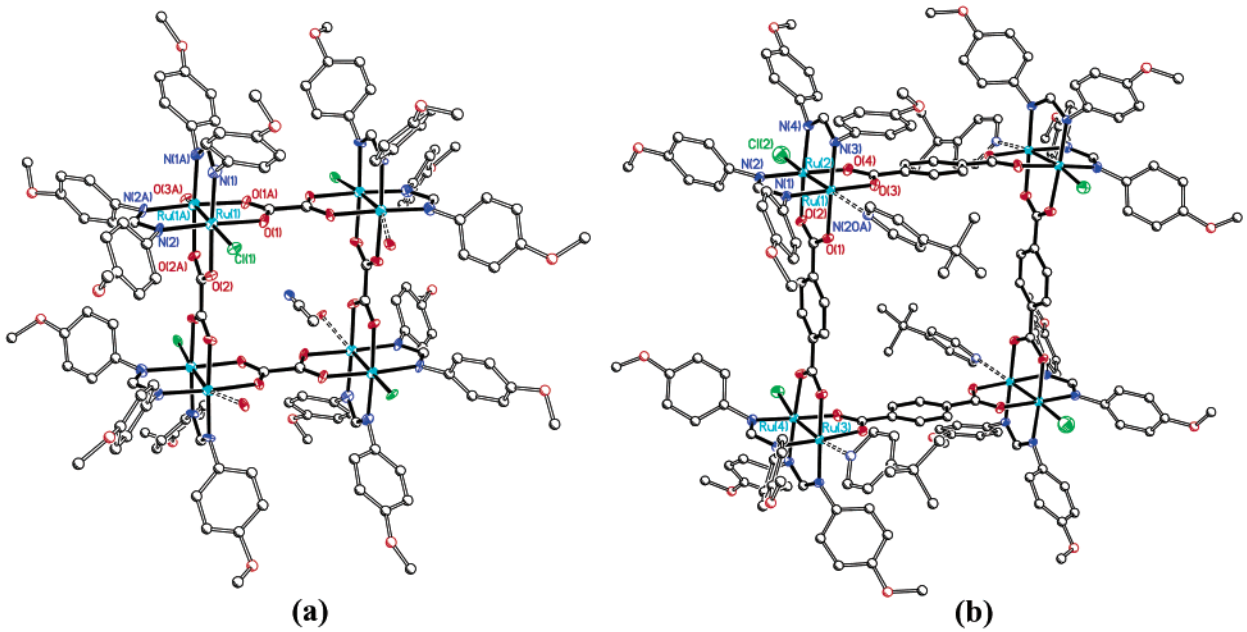

Figure 2. Perspective views of the core structures of the molecular squares **2** (a) and **3** (b). A MeCN molecule is shown inside the square cavity of **2**. Atoms are represented by thermal ellipsoids at the 30% probability level, except for carbon atoms which are shown as spheres of arbitrary radius, while hydrogen atoms are omitted for clarity.

Table 2. Selected Bond Distances (Å) and Angles (deg) for **2**

Ru(1)−Ru(1A)	2.332(2)	Ru(1)−O(2)	2.089(7)
Ru(1)−N(1)	2.04(1)	Ru(1)−Cl(1)	2.443(6)
Ru(1)−N(2)	2.04(1)	Ru(1A)···O(3A)	2.64(2)
Ru(1)−O(1)	2.087(8)		
N(1)−Ru(1)−N(2)	94.7(4)	N(1)−Ru(1)−Ru(1A)	89.5(3)
N(1)−Ru(1)−O(1)	88.8(4)	O(1)−Ru(1)−Ru(1A)	88.9(2)
N(2)−Ru(1)−O(2)	88.5(4)	N(1)−Ru(1)−Cl(1)	93.4(3)
N(1)−Ru(1)−O(2)	176.4(4)	O(1)−Ru(1)−Cl(1)	88.0(3)
N(2)−Ru(1)−O(1)	176.2(4)	Ru(1A)−Ru(1)−Cl(1)	175.7(1)
O(1)−Ru(1)−O(2)	88.0(3)	Ru(1)−Ru(1A)···O(3A)	163.0(3)

Table 3. Selected Bond Distances (Å) and Angles (deg) for **3**

Ru(1)−Ru(2)	2.332(1)	Ru(2)−N(2)	2.028(5)
Ru(1)−N(1)	2.019(5)	Ru(2)−N(4)	2.045(5)
Ru(1)−N(3)	2.021(5)	Ru(2)−O(2)	2.087(4)
Ru(1)−O(1)	2.058(4)	Ru(2)−O(4)	2.073(4)
Ru(1)−O(3)	2.078(4)	Ru(2)−Cl(2)	2.528(2)
Ru(1)···N(20A)	2.369(7)	Ru(3)−Ru(4)	2.325(1)
N(1)−Ru(1)−N(3)	93.4(2)	N(4)−Ru(2)−O(2)	176.0(2)
N(1)−Ru(1)−O(3)	177.4(2)	N(4)−Ru(2)−O(4)	88.6(2)
N(3)−Ru(1)−O(1)	176.4(2)	O(1)−Ru(1)−Ru(2)	90.5(1)
O(1)−Ru(1)−O(3)	88.4(2)	N(1)−Ru(1)−Ru(2)	89.7(1)
N(2)−Ru(2)−N(4)	88.5(2)	Ru(2)−Ru(1)···N(20A)	171.8(3)
N(2)−Ru(2)−O(2)	92.6(2)	N(4)−Ru(2)−Cl(2)	100.1(1)
N(2)−Ru(2)−O(4)	89.8(2)	O(4)−Ru(2)−Cl(2)	87.9(1)
N(2)−Ru(2)−O(2)	177.3(2)	Ru(1)−Ru(2)−Cl(2)	168.65(5)

exceptions, ordered ones. However, in the new Ru_2^{5+}-based molecular squares **2** and **3**, there are mixed axial ligands, and they are considerably disordered. Doubtless, this has something to do with the difficulties in obtaining crystals. In **2**, the two axial positions of each Ru_2^{5+} unit are occupied by disordered H_2O molecules (at a distance of 2.64(2) Å) and Cl^- anions. In **3**, besides the Cl^- anions, there are also 4-Bu^{t}py molecules (at an average distance of 2.354 Å) axially coordinated. One of the crystallographically independent Ru_2^{5+} units has a fully occupied Cl^- anion and a disordered 4-Bu^{t}py ligand coordinated axially. In the other Ru_2^{5+} unit, the axial Cl^- anion is partially

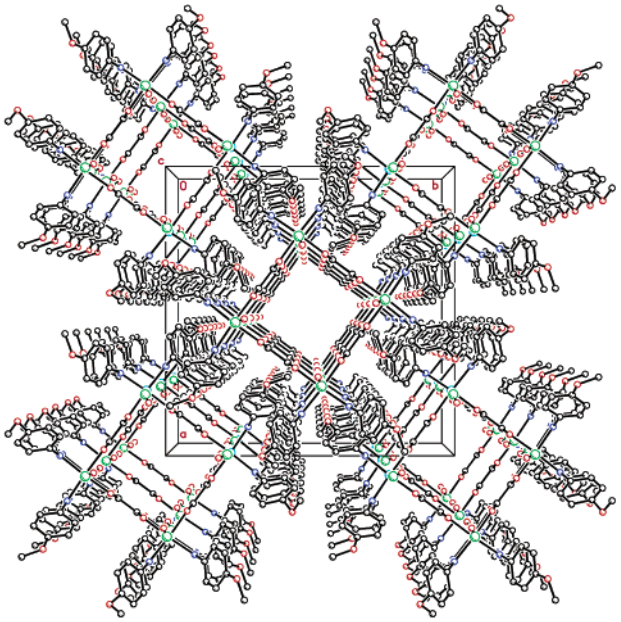

Figure 3. The rigorously tetragonal stacking of the molecules in crystals of **2**. The molecules in the center stack are at $z = 0$, and those at the corners are at $z = {}^1/_2$. All solvent molecules are omitted for clarity.

replaced by a 4-Bu^{t}py ligand; both the Cl^- anion and the 4-Bu^t-py ligand are disordered having an occupancy of 0.293 and 1.707, respectively. Thus, **3** is an ionic species in the solid state. On average, its formula can be written as $[\{cis\text{-}Ru_2(\mu\text{-DAniF})_2\text{-}Cl_{0.646}(4\text{-Bu}^t\text{py})_{1.354}\}(\mu\text{-terephthalate})]_4Cl_{1.414}\cdot 17(1,2\text{-}C_2H_4Cl_2)\cdot C_6H_{14}$.

A very interesting feature of **2** and **3** is their tendency to stack in the solid state, a property that has been previously observed in molecular squares of other dimetal units.[3] As shown in Figures 3 and 4, the molecular squares **2** and **3** stack to form square channels. The stacking arises from the way in which the *p*-anisyl groups of the DAniF ligands mesh from one layer

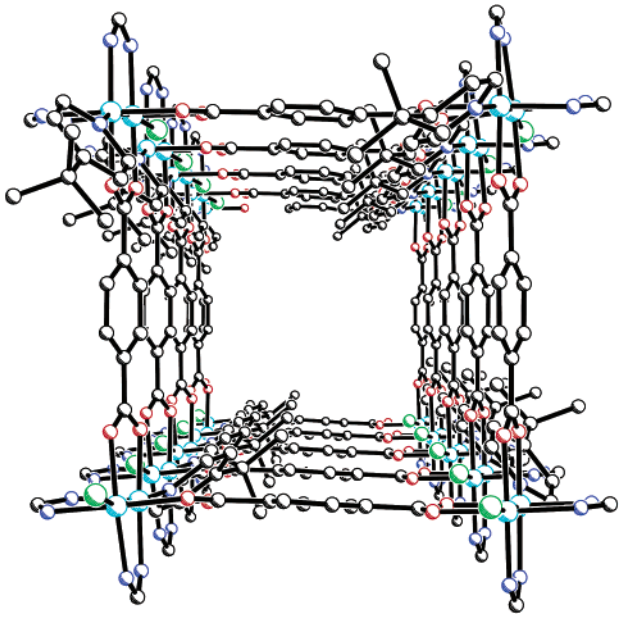

Figure 4. A stack of molecules of **3**; the *p*-anisyl groups and interstitial solvent molecules are omitted.

to adjacent ones. These square channels with widths (from one Ru_2^{5+} corner to the opposite) of ~9.5 and ~15.5 Å in **2** and **3**, respectively, are not empty; they contain moderately ordered arrays of solvent molecules: in the square cavity of **2** a disordered MeCN molecule was found (Figure 2a), whereas the larger cavity of **3** is filled with 1,2-$C_2H_4Cl_2$ and hexane molecules.

Mass Spectrometry. Positive ion electrospray ionization mass spectrometry (+ESI-MS) proved to be a valuable technique, as it offers additional evidence for the existence and the retention of the integrity of compound **1** and the molecular squares **2** and **3** in CH_2Cl_2 solutions. The +ESI mass spectrum for **1** shows only one signal at *m*/*z* 831 with an isotopic distribution consistent with the fragment $[M - Cl]^+$. The loss of a Cl^- anion is a fragmentation process which is observed very frequently in ESI spectra of Ru_2^{5+} compounds which have axially coordinated Cl^-. It was also found to be a characteristic of all of the compounds presented here, and it is in agreement with the fact that the axially coordinated Cl^- anion is only weakly bound to the Ru_2^{5+} core and easily removed. For **2**, the mass spectrum shows peaks at *m*/*z* 1636, 1080, and 801 with isotopic distributions consistent with the fragments $[M - 2Cl]^{2+}$, $[M - 3Cl]^{3+}$, and $[M - 4Cl]^{4+}$. Similarly, the mass spectrum of **3** exhibits features at *m*/*z* 1789, 1180, and 877 that can be attributed to fragments of the parent ion from which two, three, and four axially coordinated Cl^- anions have been removed. For both **2** and **3**, the singly charged fragments were not observed due to instrumental limitations. However, it can be easily concluded that the cores of the molecular squares remain essentially intact.

Electrochemistry. Compounds **1**, **2**, and **3** have been examined by both cyclic voltammetry (CV) and differential pulse voltammetry (DPV). The results of these experiments are summarized in Figure 5. The cyclic voltammogram for complex **1** displays a reversible one-electron redox process at $E_{1/2}$ = +0.734 V (E_{red}' = +0.689 and E_{ox}' = +0.778 V) which corresponds to the reaction $Ru_2^{5+} \leftrightarrow Ru_2^{6+}$. There is also an irreversible redox process with a cathodic wave at E_{red}'' = −0.747 V, which corresponds to the reduction reaction $Ru_2^{5+} \rightarrow Ru_2^{4+}$, and an anodic wave at E_{ox}'' = −0.337 V, which represents the reverse reaction $Ru_2^{4+} \rightarrow Ru_2^{5+}$.

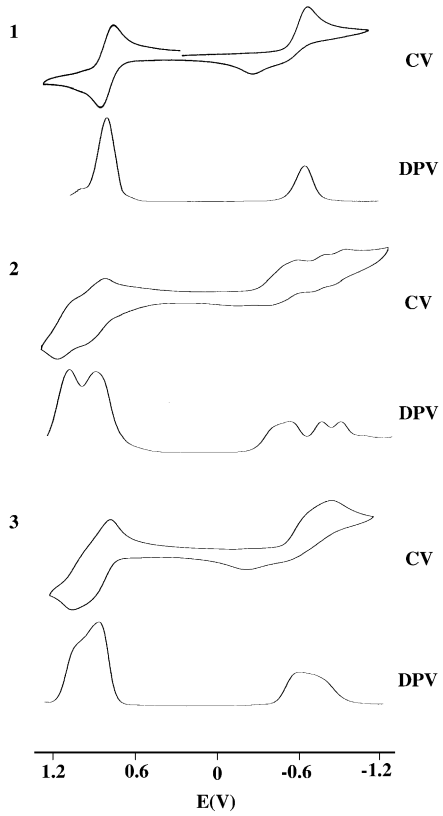

Figure 5. Cyclic and differential pulse voltammograms of **1**, **2**, and **3**.

The electrochemical behavior of the molecular squares **2** and **3** is somewhat more complicated. CV measurements show that the two compounds exhibit reversible oxidation and less reversible reduction processes. DPV for **2** shows two oxidation waves at +1.052 and +0.872 V and reduction waves at −0.480, −0.700, and −0.836 V. For **3**, DPV shows a simpler pattern with two broad and slightly split signals centered at +0.804 and −0.580 V. Due to the complexity of these redox processes, a precise estimation of the number of electrons involved cannot be obtained. However, these data are consistent with a higher degree of electronic communication between the Ru_2 units in **2**, where the shorter oxalate linkers are present.

Magnetism. Compounds **2** and **3** are based on Ru_2^{5+} corner pieces which are paramagnetic. So, these are the first paramagnetic molecular squares based on dimetal units, and they provide another probe for the communication between dimetal units in supramolecular assemblies. Thus, we decided to investigate the extent of intramolecular magnetic coupling that arises between Ru_2^{5+} units in each square. Variable temperature magnetic susceptibility measurements, Figure 6, show that the magnetic behavior for **1**, **2**, and **3** is similar near room temperature but differs significantly at lower temperatures with the value of χT of **2** being significantly lower than that of **3**. Even a simple Ru_2^{5+}species, such as the starting material *cis*-$Ru_2(\mu$-DAniF$)_2(\mu$-O_2CMe$)_2$Cl, deviates from simple Curie−Weiss behavior because of large zero-field splitting in the quartet ground state, as seen in Figure 6. The difference in the magnetic behavior of **2** and **3** relative to **1** at low temperatures is explained in terms of a weak intramolecular antiferromagnetic coupling between

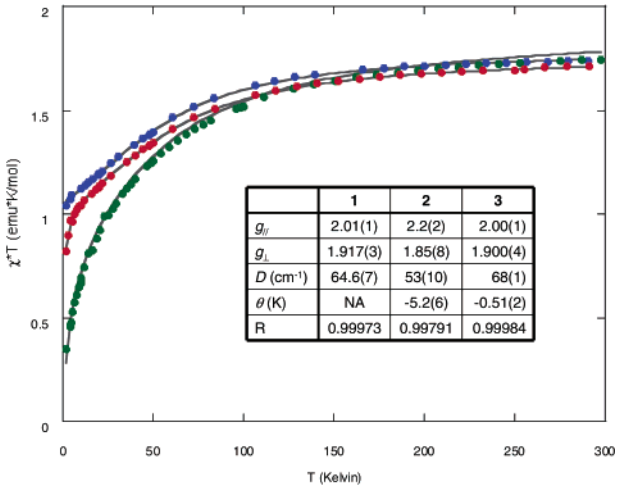

	1	2	3
$g_{\|\|}$	2.01(1)	2.2(2)	2.00(1)
$g_{\perp}$	1.917(3)	1.85(8)	1.900(4)
D (cm^{-1})	64.6(7)	53(10)	68(1)
θ (K)	NA	-5.2(6)	-0.51(2)
R	0.99973	0.99791	0.99984

Figure 6. Plots of χT per Ru_2 unit (χ represents magnetic susceptibility corrected for diamagnetism) versus temperature for **1** (blue), **2** (green), and **3** (red). The solid lines represent the theoretical fits of the data.

the paramagnetic Ru_2^{5+} centers within each square, as it is doubtful that detectable intermolecular coupling could arise between squares at distances greater than 10 Å.

From the shape of the curves of **2** and **3**, it is apparent that any intramolecular antiferromagnetic coupling is small as compared to the magnitude of the zero-field splitting (i.e., $D \gg J$). Thus, fitting of the magnetic data can be achieved by modeling the zero-field splitting and treating the anti-ferromagnetic coupling as a perturbation, as in the following zero-field Hamiltonian:

$$H = S\cdot D\cdot S - zJ\langle S_z\rangle S_z$$

From this, the zero-field splitting was worked out in a method similar to that of Telser and Drago,[25] and the second term in the Hamiltonian was approximated semiempirically by the use of a Weiss constant, giving the following expressions for the susceptibility:

$$\chi_{||} = \frac{Ng_{||}^2\beta^2}{k(T-\theta)}\cdot\frac{(1+9\exp(-2D/kT))}{4(1+\exp(-2D/kT))}$$

$$\chi_{\perp} = \frac{Ng_{\perp}^2\beta^2}{k(T-\theta)}\cdot\frac{(4+(3kT/D)(1-\exp(-2D/kT)))}{4(1+\exp(-2D/kT))}$$

The average value, given by

$$\chi = \frac{\chi_{||}+2\chi_{\perp}}{3}$$

was used to fit the data.[26] The Weiss constant was not used in the fitting of **1** (because no intermolecular interactions are proposed for this compound). The curve fits are shown in Figure 6, and the fitting parameters are given in the inset. The g factors and D parameters are reasonable in comparison to those from similar systems.[25]

Although empirical, the Weiss constant gives a crude estimate of the coupling of nearest-neighbor Ru_2 units. Thus, it is clear that, although the coupling is small, the shorter oxalate linker is a better mediator of magnetic communication than is the terephthalate linker by an order of magnitude, similar to what has been observed in other systems.[27]

The magnetic behavior of **2** and **3** may be compared to that of the molecular square $[Co(HAT)Cl_2]_4$,[28] which has four mononuclear $CoCl_2$ units linked by the nitrogen donor 1,4,5,8,9,-12-hexaazatriphenylene (HAT). In this case, the moment decrease was exclusively due to zero-field splitting of the Co atoms, and magnetic exchange was negligible.

Concluding Remarks

In an effort to synthesize a suitable Ru_2^{5+} building block for the construction of discrete paramagnetic supramolecular assemblies, the reaction between $Ru_2(\mu\text{-}O_2CMe)_4Cl$ and HDAniF was studied under different experimental conditions. As a result, a Ru_2^{5+} complex with two labile acetate groups occupying two equatorial *cisoid* positions was isolated. By using this compound as starting material in carboxylate exchange reactions with two linear dicarboxylic acids, oxalic acid and terephthalic acid, we have prepared the first molecular squares with Ru_2^{5+} corner pieces. Because each of the Ru_2^{5+} units has 3 unpaired electrons, the resulting molecular squares are paramagnetic and have 12 unpaired electrons. The magnetic and electronic communication between the Ru_2^{5+} centers in these entities has been studied. As expected, oxalate linkers are better than the terephthalate linkers in effecting electronic and magnetic coupling; however, even for the oxalate, the near neighbor coupling is small in comparison to the temperature dependence inherent in each Ru_2^{5+} unit due to zero-field splitting.

This work represents the first step toward the goal of Ru_2^{5+}-based single molecule magnets by introducing a strategy for the synthesis of robust supramolecules. We believe that, using appropriate linkers, it will be possible in the future to synthesize $(Ru_2^{5+})_n$ macrocycles with ferromagnetic interactions (or ferrimagnetic if the linkers contain unpaired spins). This possibility, along with the molecular and magnetic anisotropy of these compounds, signifies the potential for single molecule magnet behavior. Also, these assemblies could be conducting if the Ru_2 units can be linked together by axial linkers. Conducting supramolecular assemblies are known,[29] but none of these take advantage of direct metal−metal bonds as we propose here. In short, with the synthesis of **1**, **2**, and **3**, we have opened the door to the possibility of magnets and conductors built with metal−metal bonded subunits.

Experimental Section

All reactions and manipulations were performed under a nitrogen atmosphere, using standard Schlenk line techniques. Commercial grade solvents were dried and deoxygenated by reflux under an N_2 atmosphere for at least 24 h over appropriate drying agents and were freshly distilled prior to use. $Ru_2(\mu\text{-}O_2CMe)_4Cl$ was prepared as described in the

(25) (a) Telser, J.; Drago, R. S. *Inorg. Chem.* **1984**, *23*, 3114. (b) Telser, J.; Miskowski, V. M.; Drago, R. S.; Wong, N. M. *Inorg. Chem.* **1985**, *24*, 4765.
(26) Similar methods have been used to fit chans of linked Ru_2^{5+} units: (a) Miyasaka, H.; Clérac, R.; Campos-Fernández, C. S.; Dunbar, K. R. *Inorg. Chem.* **2000**, *40*, 1663. (b) Cukiernik, F. D.; Luneau, D.; Marchon, J.-C.; Maldivi, P. *Inorg. Chem.* **1998**, *37*, 3698. (c) Jiménez-Aparicio, R.; Urbanos, F. A.; Arrieta, J. M. *Inorg. Chem.* **2001**, *40*, 613.
(27) See, for example: (a) Sun, D.; Cao, R.; Liang, Y.; Shi, Q.; Su, W.; Hong, M. *J. Chem. Soc., Dalton Trans.* **2001**, 2335. (b) Armentano, D.; DeMunno, G.; Faus, J.; Lloret, F.; Julve, M. *Inorg. Chem.* **2001**, *40*, 655.
(28) Galán-Mascarós, J. R.; Dunbar, K. R. *Chem. Commun.* **2001**, 217.
(29) Akutagawa, T.; Hasegawa, T.; Nakamura, T.; Inabe, T. *J. Am. Chem. Soc.* **2002**, *124*, 8903.

Table 4. Crystal Data and Refinement Parameters for **1**, **2**, and **3**

	1	**2**	**3**
empirical formula	$C_{34}H_{38}ClN_4O_9Ru_2$	$C_{142}H_{183}Cl_{14}N_{17}O_{48}Ru_8$	$C_{240.72}H_{288.38}Cl_{38}N_{21.41}O_{32}Ru_8$
fw	884.27	3846.41	6149.40
space group	$P2_1/n$	$I4/m$	$P\bar{1}$
a (Å)	12.2674(9)	19.916(1)	19.208(1)
b (Å)	19.963(1)	19.916(1)	20.616(1)
c (Å)	14.324(1)	25.760(4)	22.578(1)
α (deg)	90	90	89.698(1)
β (deg)	100.39(1)	90	66.277(1)
γ (deg)	90	90	70.313(1)
V (Å^3)	3450.5(4)	10217(2)	7618.4(8)
Z	4	2	1
ρ_{calc} (g cm^{-3})	1.702	1.250	1.340
μ (mm^{-1})	1.014	0.694	0.778
λ (Å)	0.71073	0.71073	0.71073
T (K)	213(2)	213	193
R1, wR2 ($I > 2\sigma(I)$)[a]	0.0295, 0.0660	0.0820, 0.1973	0.0652, 0.1724
goodness-of-fit	1.029	1.147	1.096

[a] $R1 = \sum||F_o| - |F_c||/\sum|F_o|$. $wR2 = [\sum[w(F_o^2 - F_c^2)^2]/\sum[w(F_o^2)^2]]^{1/2}$, $w = 1/\sigma^2(F_o^2) + (aP)^2 + bP$, where $P = [\max(0 \text{ or } F_o^2) + 2(F_c^2)]/3$.

literature.[30] HDAniF was prepared according to the published general procedure for the synthesis of formamidines.[31] Oxalic acid, terephthalic acid, and 4-Bu^{t}py were purchased from Aldrich and used as received.

Mass spectrometry data (electrospray ionization) were recorded at the Laboratory for Biological Mass Spectrometry at Texas A&M University, using an MDS Series Qstar Pulsar with a spray voltage of 5 keV. IR spectra were recorded in a Perkin-Elmer 16PC FT IR spectrophotometer as KBr pellets. CV and DPV measurements were carried out on a CH Instruments model CH1620A electrochemical analyzer, with Pt working and auxiliary electrodes, and a Ag/AgCl reference electrode. The scan rate was 0.1 V/s for CV and 0.002 V/s for DPV. The $E_{1/2}$ values for CV were obtained from the relationship $E_{1/2} = (E_a + E_c)/2$, while for DPV they were obtained from the relationship $E = E_p + E_{pul}/2$, $E_{pul} = 0.05$ V. The experiments were performed at room temperature under nitrogen atmosphere, in CH_2Cl_2 solutions that contained 0.1 M (Bu^n_4N)(PF_6) as supporting electrolyte. All of the potentials were referenced to the Ag/AgCl electrode, and, under our experimental conditions, the $E_{1/2}$ for the Fc/Fc$^+$ couple occurred at +0.440 V. Variable temperature magnetic susceptibility measurements were obtained with the use of a Quantum Design SQUID magnetometer MPMS-XL at 1000 G, and the data were corrected for diamagnetism.

Syntheses. *cis*-Ru$_2$(μ-DAniF)$_2$(μ-O$_2$CMe)$_2$Cl (1). To a mixture of 0.157 g (0.330 mmol) of Ru$_2$(μ-O$_2$CMe)$_4$Cl and 0.211 g (0.820 mmol) of HDAniF was added a 15 mL portion of THF. The brown suspension was stirred and refluxed gently for 18 h, resulting in a color change to dark purple. After some unreacted Ru$_2$(μ-O$_2$CMe)$_4$Cl was filtered off, the solvent was removed under vacuum leaving a dark residue. The residue was dissolved in 4−5 mL of MeCN and precipitated by addition of a mixture of 20 mL of Et$_2$O and 70 mL of hexanes. The supernatant liquid was removed by cannula filtration, and the solid was dried under vacuum for 30 min. This procedure was repeated twice. The product was purified by column chromatography (silica gel; eluent (v/v): CH_2Cl_2/acetone = 5/2). A green-purple solid was isolated. Dark green-purple crystals of **1**·H$_2$O were obtained over a period of 2−3 days by layering hexanes over a CH_2Cl_2 solution of the product. Yield: 0.110 g (40%). +ESI-MS (CH_2Cl_2, m/z): 831 ([M − Cl]$^+$). IR (KBr disk, cm^{-1}): 460 (w), 545 (w), 594 (w), 693 (m), 770 (w), 835 (m), 1034 (m), 1109 (w), 1177 (m), 1216 (s), 1247 (s), 1297 (m), 1316 (m), 1438 (s), 1500 (s), 1529 (s), 1605 (m), 2835 (w), 2938 (w), 3447 (m). CV (V vs Ag/AgCl): $E_{1/2} = +0.734$ V ($E_{red}' = +0.689$ and $E_{ox}' = +0.778$ V), $E_{red}' = -0.747$ V, $E_{ox}' = -0.337$ V.

[{*cis*-Ru$_2$(μ-DAniF)$_2$Cl(H$_2$O)}(μ-oxalate)]$_4$·MeCN·2(C$_6$H$_{14}$)·12H$_2$O (2). To a mixture of 0.15 g (0.17 mmol) of *cis*-Ru$_2$(μ-DAniF)$_2$(μ-O$_2$CMe)$_2$Cl and 0.016 g (0.18 mmol) of oxalic acid was added 10 mL of dry toluene. The reaction mixture was stirred and refluxed for 48 h, resulting in a purple precipitate. The mixture was allowed to cool, and it was filtered. The solid was washed with toluene, extracted with CH_2Cl_2, and filtered again. Addition of hexanes gave a precipitate that was collected. Crystals suitable for X-ray diffraction were obtained over a period of 2 weeks by layering hexanes over a 1,2-$C_2H_4Cl_2$ solution of the Ru$_2$ square to which a few drops of MeCN and traces of H$_2$O had been added. Yield: 0.104 g (72%). +ESI-MS (CH_2Cl_2, m/z): 1636 ([M − 2Cl]$^{2+}$), 1080 ([M − 3Cl]$^{3+}$), 801 ([M − 4Cl]$^{4+}$). IR (KBr disk, cm^{-1}): 424 (w), 471 (w), 595 (w), 728 (w), 795 (w), 832 (m), 946 (w), 1029 (m), 1108 (w), 1179 (m), 1216 (s), 1248 (s), 1297 (s), 1383 (w), 1465 (w), 1501 (s), 1575 (s), 1635 (s), 1700 (m), 1734 (w), 1942 (w), 2836 (w), 2956 (w), 3447 (m). DPV (CH_2Cl_2, 22 °C, V vs Ag/AgCl): $E_{red}' = -0.480$ V, $E_{red}' = -0.702$ V, $E_{red}' = -0.848$ V, $E_{ox}' = +0.867$ V, $E_{ox}' = +1.044$ V.

[{*cis*-Ru$_2$(μ-DAniF)$_2$Cl$_{0.646}$(4-Bu^{t}py)$_{1.354}$}(μ-terephthalate)]Cl$_{1.414}$·17(1,2-C$_2$H$_4$Cl$_2$)·C$_6$H$_{14}$ (3). To a mixture of 0.15 g (0.17 mmol) of *cis*-Ru$_2$(μ-DAniF)$_2$(μ-O$_2$CMe)$_2$Cl and 0.031 g (0.19 mmol) of terephthalic acid was added 10 mL of dry toluene. The reaction mixture was stirred and refluxed for 48 h, resulting in a purple precipitate. The mixture was allowed to cool, and it was filtered. The solid was washed with toluene, extracted with CH_2Cl_2, and filtered again. Addition of Et$_2$O gave a precipitate that was collected. Crystals suitable for X-ray structure analysis were obtained over a period of 3−4 days by layering hexanes over a 1,2-$C_2H_4Cl_2$ solution of the Ru$_2$ square to which a few drops of 4-Bu^{t}py had been added. Yield: 0.088 g (56%). +ESI-MS (CH_2Cl_2, m/z): 1789 ([M − 2Cl]$^{2+}$), 1180 ([M − 3Cl]$^{3+}$), 877 ([M − 4Cl]$^{4+}$). IR (KBr disk, cm^{-1}): 463 (w), 581 (w), 690 (w), 741 (w), 805 (w), 838 (m), 1035 (s), 1108 (w), 1171 (m), 1217 (m), 1246 (s), 1298 (w), 1395 (s), 1443 (s), 1474 (s), 1502 (s), 1528 (m), 1605 (s), 2492 (s), 2530 (w), 2623 (s), 2677 (s), 2738 (s), 2938 (s), 2975 (s), 3446 (w). DPV (CH_2Cl_2, 22 °C, V vs Ag/AgCl): $E_{red}' = -0.580$ V, $E_{ox}' = +0.804$ V.

X-ray Crystallography. Specimens of suitable quality and size of **1**−**3** were mounted on the ends of quartz fibers and used for intensity data collection on a Bruker SMART 1000 CCD area detector system equipped with a liquid nitrogen low-temperature controller using Mo Kα radiation. Cell parameters were obtained using SMART software.[32] Data reduction and integration were performed using the software package SAINT PLUS,[33] which also corrects for Lorentz and polarization effects, while absorption corrections were applied using the program

(30) Stephenson, T. A.; Wilkinson, G. *Inorg. Nucl. Chem.* **1966**, *28*, 2285.
(31) Roberts, R. M. *J. Org. Chem.* **1949**, *14*, 277.
(32) *SMART*. Data Collection Software, Version 5.618; Bruker Analytical X-ray Systems, Inc.: Madison, WI, 2000.
(33) *SAINTPLUS*. Data Reduction Software, Version 6.28A; Bruker Analytical X-ray Systems, Inc.: Madison, WI, 2001.

SADABS.[34] In all structures, the positions of heavy atoms were found via direct methods using the SHELXTL software.[35] Subsequent cycles of least-squares refinement, followed by difference Fourier syntheses, revealed the positions of the remaining non-hydrogen atoms. All non-hydrogen atoms, except for the disordered ones, were refined anisotropically. Hydrogen atoms were placed at idealized calculated positions. Cell parameters and basic information pertaining to data collection and structure refinement for compounds **1**−**3** are summarized in Table 4.

(34) *SADABS*. Area Detector Absorption and other Corrections Software, Version 2.03; Bruker Analytical X-ray Systems, Inc.: Madison, WI, 2000.
(35) Sheldrick, G. M. *SHELXTL*. Version 6.10, Bruker Analytical X-ray Systems, Inc.: Madison, WI, 2000.

Acknowledgment. We thank the National Science Foundation for financial support. J.F.B. is grateful to the National Science Foundation for a predoctoral fellowship.

Supporting Information Available: X-ray crystallographic data in CIF format for **1**, **2**, **3**, and *cis*-$Ru_2(\mu\text{-DTolF})_2(\mu\text{-}O_2\text{-}CMe)_2Cl(HN{=}CH{-}NH{-}C_6H_4{-}p\text{-Me})$. This material is available free of charge via the Internet at http://pubs.acs.org.

JA036095X